

1-1-2013

Spliceosomal Prp24 Unwinds A Minimal U2/u6 Complex From Yeast

Chandani Manoja Warnasooriya
Wayne State University,

Follow this and additional works at: http://digitalcommons.wayne.edu/oa_theses

 Part of the [Biochemistry Commons](#), and the [Chemistry Commons](#)

Recommended Citation

Warnasooriya, Chandani Manoja, "Spliceosomal Prp24 Unwinds A Minimal U2/u6 Complex From Yeast" (2013). *Wayne State University Theses*. Paper 249.

This Open Access Thesis is brought to you for free and open access by DigitalCommons@WayneState. It has been accepted for inclusion in Wayne State University Theses by an authorized administrator of DigitalCommons@WayneState.

**SPLICEOSOMAL PRP24 UNWINDS A MINIMAL U2/U6 COMPLEX
FROM YEAST**

by

CHANDANI MANOJA WARNASOORIYA

THESIS

Submitted to the Graduate School

of Wayne State University,

Detroit, Michigan

in partial fulfillment of the requirements

for the degree of

MASTER OF SCIENCE

2013

MAJOR: CHEMISTRY (Biochemistry)

Approved By:

Co-Advisor Date

Co-Advisor Date

DEDICATION

To My Loving Family and Husband

ACKNOWLEDGEMENTS

First of all I want to convey my sincere gratitude to my advisor, Dr David Rueda, for giving me the opportunity to work in his lab, which opens the path to learn an emerging technique and his guidance, encouragement and support throughout my research work. I'm fortunate to be a part of his lab and able to do promising research. Thank you very much Dr. Rueda for all the help and opportunities you have given me, and for the diligent effort you made to train me as a good scientist.

I would also like to thank my thesis committee, Dr. Louis Romano and Dr. Arthur Suits, for their valuable suggestions and feedback on my research. My special thanks go to Dr. Christine Chow for her cooperation, guidance and support through my difficult times. I am also thankful to our collaborators Dr. Samuel Butcher, Dr. David Brow and Ashley Richie from University of Wisconsin-Madison for sending me the Prp24 protein and important discussions and suggestions.

Then, I would like to acknowledge all my lab members. My biggest thank goes to Zhuojun Guo for teaching me single molecule experiments and everything not only about research but also about life. Thank you so much Zhuojun for everything you taught me and for the fun times we had in the lab. I also want to give a big thanks to Dr. Amanda Solem for her continuous support and valuable suggestions and Dr. Elvin Aleman and Dr. Alfonso Brenlla for the technical support in single molecule setup. I also want to thank my former lab mates Rajan, Krishanthi, Rui, Sharla, May and Marcus for their immense guidance and support. I would also want to thank my fellow lab mates, Bishnu, Hansini, Imali, Eric, Pramodha and Gayan for the valuable discussions we had

and making the stressful graduate school life an endurable one. I also like to thanks Chow lab members for their help for my research, especially Gayani and Daya for helping me with MALDI and Xun for encouraging me and cheering me up in my difficult times.

I want to convey my sincere appreciation to Chemistry department administrative staff specially Melissa Nestor, Debbie, Diane and all the others.

I would also like to thank Wayne state - Sri Lankan student Association, Michigan Sri Lankan community and all my Sri Lankan friends, who help me to make a second home in USA. I'm thanking to all my best friends in Sri Lanka who were there for me to cheer me up and help me.

Finally, I would like to convey my heartfelt appreciation to my Parents; Upali Warnasooriya and Chandra Warnasooriya for bringing me up as a better human and for everything you did throughout my life. Also I thank to my brother Vindana and sister-in-law Pradeepa for encouraging me and also for taking care of our parents while I'm far away from them. Your love means a lot to me, especially to bear this stressful life in a foreign country. Last but not least I want to express my utmost gratitude to my loving husband Chinthaka Sanjeewa for his enormous support, encouragement and love which means so much for me. Since the day we met, you were there by my side for last 8 years, helping me in every way to fulfill my dreams and come this far in my career. Without your love, protection and guidance, I can't imagine how I would have come this far. Thank you very much for being with me in every step in my life and I'm sorry for all the hardship you have to face while you are helping me to accomplish my dreams.

LIST OF CONTENTS

DEDICATION.....	ii
ACKNOWLEDGEMENTS.....	iii
LIST OF FIGURES	vii
CHAPTER 1: Introduction.....	1
1.1: Pre-mRNA splicing catalyzed by the spliceosome	1
1.2: U2-U6 complex makes the catalytic core of the spliceosome and adopts multiple conformations.....	4
1.3: Role of spliceosome-associated proteins in splicing.....	7
1.4: Prp24 is an U6 associated chaperone.....	8
1.5: Defects in splicing and spliceosomal components can be lethal	10
CHAPTER 2: Material and Methods	13
2.1: Sample purification and labeling.....	13
2.2: MALDI-MS experiments	14
2.3: Fluorescence anisotropy experiments.....	15
2.4: Gel-shift assays	16
2.5: Single-molecule experiments	17

CHAPTER 3: Results and Discussion	19
3.1: Gel shift assay and fluorescence anisotropy measurements reveal binding of Prp24 with yeast minimal U2/U6 construct.....	20
3.2: Presence of Prp24 affects the structural dynamics of U2/U6 complex	23
3.3: Effect of RRM1s on the binding of Prp24 with U2/U6 complex.....	25
3.4: Binding of Prp24 facilitates the unwinding of U2 from the complex	29
CHAPTER 4: Conclusions and future directions.....	34
REFERENCES.....	37
ABSTRACT	45
AUTOBIOGRAPHICAL STATEMENT	47

LIST OF FIGURES

Figure 1: Two transesterification reactions occur during splicing.	2
Figure 2: Assembly and catalysis of the spliceosome.....	3
Figure 3: Highly conserved regions in U6 and alternative conformations of U2/U6 complex are important for the spliceosomal assembly and catalysis	5
Figure 4: Proposed folding reaction pathway of the U2/U6 complex.....	7
Figure 5: Prp24 acts as a U6 chaperone.....	9
Figure 6: Single molecule experimental setup for U2/U6 complex with Prp24.....	11
Figure 7: MALDI result reveals the mass of the fragment that is used for Cy5 labeling.....	15
Figure 8: Structural dynamics of the U2/U6 complex in the absence of Prp24.....	19
Figure 9: Prp24 binds to U2/U6 complex.....	21
Figure 10: Binding of Prp24 with the U2/U6 complex stabilizes the low FRET conformation.	24
Figure 11: of full-length Prp24 (a) and truncated 234C (c) on the conformational dynamics of U2/U6.....	26
Figure 12: Prp24 induces unwinding of U2 from the complex	30
Figure 13: Binding of Prp24 facilitates the removal of U2.....	32
Figure 14: The proposed model for the role of Prp24 on the conformational dynamics of U2/U6 complex.....	33

CHAPTER 1: Introduction

1.1: Pre-mRNA splicing catalyzed by the spliceosome

Splicing plays a major role in eukaryotic gene expression by processing pre-mRNA to form mature mRNA.¹⁻³ It provides a mechanism for maintenance of the mRNA level, which helps cells to regulate gene expression.⁴ Similarly, alternative splicing plays an important role in protein diversity in cells by forming multiple mature mRNAs from a single pre-mRNA.⁵⁻⁷ Splicing involves excision of introns, which are the non-protein coding regions from nuclear pre-mRNA and religation of the protein coding regions known as exons to produce mature mRNA.^{1,2} This process occurs via two transesterification reactions. In the first reaction, the 5'-splice site cleaves and produces a 2'-5' phosphodiester linkage between the 5' end of the intron and the 2' OH of an adenine residue close to the 3' end of the intron (referred as the branch point) (Figure 1). This reaction results in a free 3' OH at the 5' exon and a circular lariat intermediate. Secondly, cleavage of the 3'-splice site occurs followed by religation of the two exons and removal of the lariat structure.^{2,8}

Splicing is catalyzed by the spliceosome, a multi-mega-dalton ribonucleoprotein complex.² Two types of spliceosomes have been reported to be present in organisms. These are the U2-dependent major and U12-dependent minor spliceosomes.^{9,10} The major spliceosome splices the highly abundant U2-type introns, whereas the minor spliceosome splices the less abundant U12-type introns¹¹. Both spliceosomes consist of five small nuclear ribonucleoproteins (snRNPs) and numerous non-snRNP proteins^{2,9}. Each snRNP consists of a small nuclear RNA (snRNA), several snRNP-specific

proteins, and a common set of proteins called sm-proteins^{2,8}. The major spliceosome of yeast, which is the focus of this study, consists of five snRNAs known as U1, U2, U4, U5 and U6 and more than 70 proteins.^{12,13}

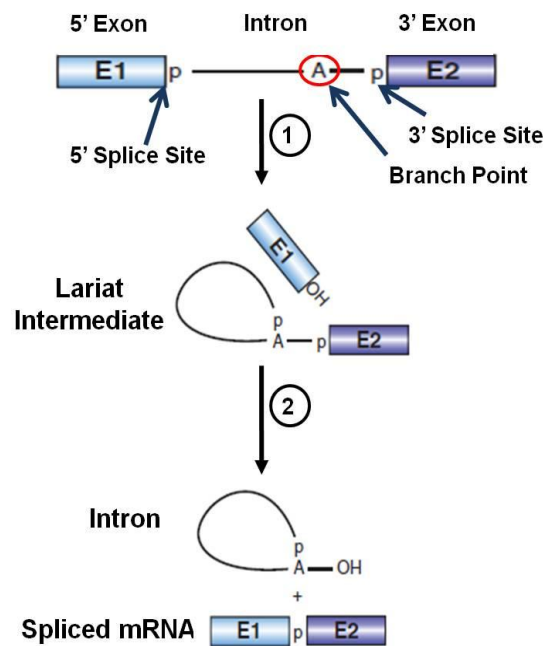


Figure 1: Two transesterification reactions occur during splicing.² First, the 5'-splice site cleaves and produces a 2'-5' phosphodiester linkage between the 5' end of intron and the 2' OH of the branch site adenosine (circled in red) resulting in a lariat intermediate and a free 5' exon. Secondly, the 3'-splice site is cleaved and the two exons are ligated together followed by removal of the lariat structure.

SnRNAs and related protein factors repeatedly undergo a highly ordered and stepwise pathway during the spliceosomal assembly and catalysis (Figure 2).² First, the U1 snRNP recognizes the 5' splice site in the pre-mRNA and U2 binds to the branch point, subsequently forming the pre-spliceosome (complex A). The U4/U6 di-snRNP associates with U5 to form the U4/U6•U5 tri-snRNP complex. This preformed tri-snRNP binds to the pre-mRNA to form the pre-catalytic spliceosome (complex B). This binding causes major structural rearrangements within RNA-RNA and RNA-protein interactions

which results in the release of U1 and U4 from the complex and forming the activated spliceosome (complex B^{act}). The B^{act} complex is further activated by ATP-dependent helicases to form the B* complex, which catalyzes the first step of splicing. This gives rise to complex C, which catalyzes the second catalytic step. After both steps of splicing have occurred and the mature mRNA is formed, the spliceosomal components dissociate and start another cycle of splicing.^{1-3,8} During the splicing reaction, only U2, U5 and U6 remain in the spliceosome, and thus it has been suggested that they form the catalytic core of the splicing machinery.^{7,14} Assembly of the spliceosomal components and their recycling after both splicing reactions are highly conserved.²

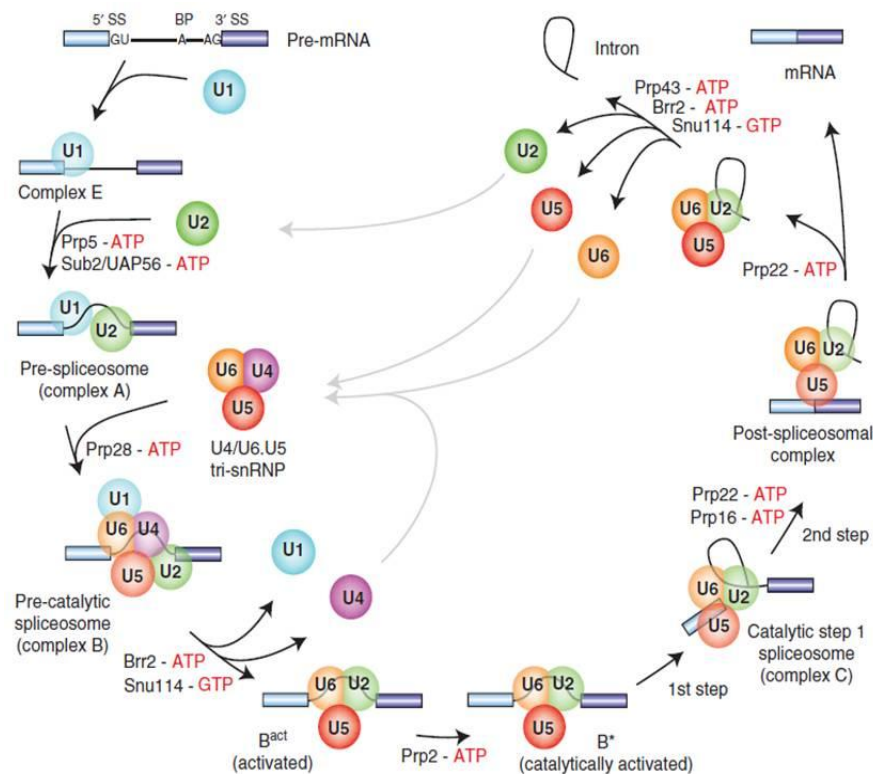


Figure 2: Assembly and catalysis of the spliceosome.² The stepwise assembly of the five snRNPs (circles) on premRNA (exons as boxes and intron as a black line, respectively) and involvement of different proteins at each step are shown.

1.2: U2-U6 complex makes the catalytic core of the spliceosome and adopts multiple conformations

Although splicing requires the assembly of all five snRNPs, only U2, U5 and U6 have been shown to be present in the catalytically active spliceosome.² Previous studies have also shown that U5 is functionally dispensable from both steps of splicing.^{15,16} All these findings have led to the suggestion that the U2/U6 complex is responsible for the catalysis and it acts as the active site of the spliceosome. This has been demonstrated in studies done with protein-free U2/U6 complexes, which are able to catalyze reactions similar to both steps of splicing.^{17,18}

There are many similarities between the group II intron, another type of intron that undergoes self-splicing, and the RNA-based catalysis of the spliceosome.^{19,20} Both systems use similar reaction mechanisms in splicing.¹⁹ Also, the catalytically important domain (D5) in the group II intron has many similarities with the U6 snRNA. The intramolecular stem loop (ISL) in U6 is similar to D5 in the group II intron.²⁰ They both share similar conserved residues, such as the metal ion binding bulge and the catalytic triad (Figure 3).^{20,21} These structural similarities have led to suggestions that U6 plays an important role in the catalytic core of the spliceosome.²² The U6 has also been suggested to be the most structurally dynamic spliceosomal RNA. In order to enter into the spliceosomal cycle, U6 needs to be paired with the U4 snRNA, and thus the U6 intramolecular stem-loop (ISL) has to be unwound. Later on, the ISL should be reformed when U6 base pairs with U2 and form the catalytically active complex.^{23,24} Therefore, this dynamic nature of U6 is believed to be very crucial for the spliceosomal assembly and catalysis. The highly conserved regions (from yeast to human) in U6 snRNA, such

as the metal ion binding U80, the AGC triad, and the ACAGAGA loop, are suggested to form a base-pairing network between U2 and the pre-mRNA, resulting in the formation of the catalytic core of the spliceosome.^{25,26} During the formation of the activated complex, U6 replaces U1 and interacts with the 5' splice site via the ACAGAGA loop.^{27,28} U5 interacts with 3' and 5' exons via its stem-loop I structure.^{15,29} U2 remains in contact with the branch site. It has been proposed that base pairing between U2 and U6 allows the 5' splice site and the branch site adenosine to juxtapose and bring the metal-ion binding site closer which is crucial for the catalysis.^{2,16,26}

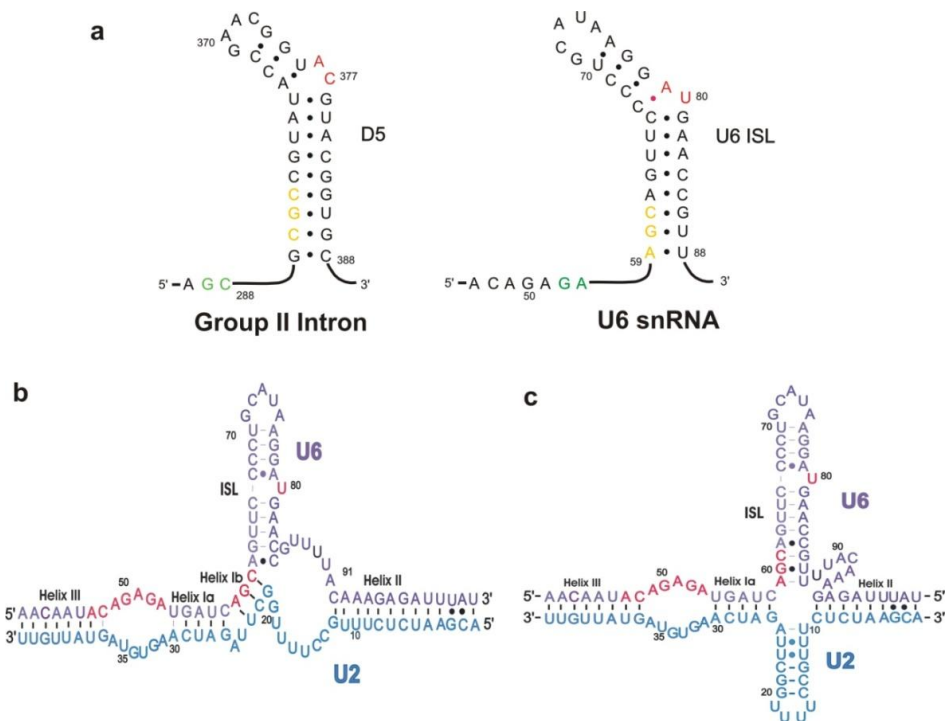


Figure 3: Highly conserved regions in U6 and alternative conformations of U2/U6 complex are important for the spliceosomal assembly and catalysis. **(a)** Structural similarities between catalytic site of group II intron D5 and U6 snRNA. Catalytic triad and metal ion binding bulge are shown in yellow and red, respectively. **(b)** The three-helix junction proposed by the Guthrie lab³⁰ and recently published NMR data by Butcher lab.³¹ In this structure, the invariant AGC triad of U6 forms intermolecular base pairs with U2. **(c)** Four-helix junction proposed by the Manley lab³² and Butcher lab²⁵. This structure suggests AGC triad form intramolecular base pairing with U6 resulting an extended ISL (Highly conserved regions of U6 snRNA are shown in red).

The catalytically important conformation of the U2/U6 complex has been in debate for many years.² According to the genetic studies done by Guthrie lab³⁰, and recent NMR studies done by Butcher lab³¹ the AGC triad of U6 base pairs with a region in U2 and forms a three-helix structure consisting of helix Ia, Ib, and III. Mammalian genetic studies done by the Manley lab³² and recent NMR studies done by Butcher lab²⁵, have proposed a four-helix structure, in which the AGC triad base pairs with U6 itself and forms an extended ISL (Figure 3). Single-molecule fluorescence resonance energy transfer (sm-FRET) studies carried out in our lab have shown that the minimal U2/U6 complex from yeast can adopt at least three distinct conformations in dynamic equilibrium, corresponding to three distinct FRET states, 0.2, 0.4 and 0.6, as a function of Mg^{2+} concentration (Figure 4).³³ At zero or very low Mg^{2+} concentrations, the U2/U6 complex adopts a conformation corresponding to a high FRET value (0.6), whereas at high Mg^{2+} concentrations, it forms the low FRET (0.2) conformation.³³ The intermediate FRET value (0.4) corresponds to an intermediate conformation. Furthermore, it has also been proposed that there is formation of base-triple interactions within U6 snRNA, involving the ACAGAGA loop, AGC triad and U80³⁴. At low Mg^{2+} concentrations, U80 tends to flip out and favors the formation of the base triple interactions, which bring the ACAGAGA loop closer to U80 and results in a high FRET state. In high Mg^{2+} concentrations, U80 stacks in the U6 ISL and disrupts base triples, resulting a low FRET state (Figure 4).³⁴ These results support the notion that the 5' splice site and the branch-site adenosine are juxtaposed, and bring the metal-ion binding site closer for the catalysis.^{16,26} Overall, these results suggest that the dynamic nature of the spliceosome between different structures is important for its assembly and the splicing reaction.²

1.3: Role of spliceosome-associated proteins in splicing

Other than the snRNPs, the spliceosome also associates with several protein factors in order to have optimum catalytic activity.^{2,8,12} During assembly and catalysis, the spliceosomal components undergo various conformational changes that are crucial for its activity. Most of the proteins that are required for such rearrangements belong to the family of DExD/H-box-type ATPase-dependent RNA helicases and ATPase-independent RNA chaperons.^{1,12} These proteins play a major role in the structural rearrangements of the spliceosomal components by helping to unwind, anneal, or stabilize the RNA components in order to form the active complex.^{1,30} Also, binding of some proteins may prevent the premature formation of certain conformations of snRNAs important for the catalysis or proper assembly of the spliceosome.^{1,2} One of such group of proteins is the “Prp” (pre-mRNA processing protein) group. There are several Prp proteins involve in the spliceosomal assembly, including Prp8, Prp16, and Prp24.

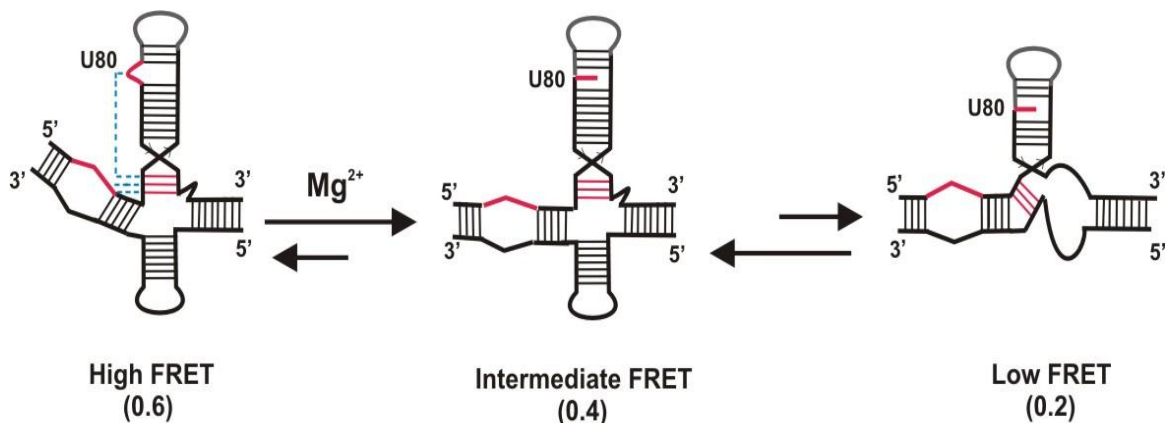


Figure 4: Proposed folding reaction pathway of the U2/U6 complex. In the absence or low $[Mg^{2+}]$, the U2/U6 complex adopts a high FRET (0.6) conformation by the formation of base-triple interactions (blue dash lines) between the highly conserved ACAGAGA loop, AGC triad, and U80 (red). Binding of Mg^{2+} induces a conformational change in the U2/U6 complex by disrupting the base-triple interaction and eventually stabilizes a low FRET (0.2) conformation via an intermediate (corresponding to 0.4 FRET).^{33,34}

1.4: Prp24 is an U6 associated chaperone

The spliceosomal protein, Prp24 plays a major role in the spliceosomal assembly. The Prp24 is thus an essential component of the U6 snRNP and it's considered as the RNA chaperone of U6, since it does not hydrolyze ATP.^{23,35-39} Studies on Prp24 have suggested that it helps U6 to remodel the catalytically important structure.^{40,41} Prp24 accelerates the annealing of U4 and U6, allowing U6 to enter into the assembly pathway.⁴² Prp24 binds to U6 as well as with Lsm ('like sm') proteins, another member of the U6 snRNP.³⁶ It has been shown that after formation of the U4/U6 complex, Prp24 leaves the complex and helps to re-anneal two snRNAs for the next cycle of assembly, suggesting its role as a recycling factor.^{42,43} Some studies proposed that Prp24 returns during the activation of the spliceosome, in which it is involved in the unwinding of U4, allowing U6 to bind with U2 to form the catalytically activated complex.⁴⁴⁻⁴⁶ Tight binding of Prp24 to U6, but not with U4, has lead to the proposal that Prp24 may also play other roles in spliceosomal assembly, such as helping to stabilize free U6 until it's ready to bind with U2 to form the active complex, after helping to dissociate U4/U6. In other words, Prp24 may prevent the premature formation of the active conformation of U6 snRNA.^{40,44,45}

Prp24 is a 51-kDa protein, present in eukaryotes, from yeast to human, and consists of four RNA recognition motifs (RRMs) (Figure 5a).^{35,47} Crystal structure studies have shown that the first three RRMs fold canonically with a $\beta\alpha\beta\beta\alpha\beta$ folding pattern.³⁵ The structure of the fourth RRM4 has been determined in a recent study and suggested that it folds non-canonically, in which it has additional flanking α -helices compared to the canonical RRM-fold, thus it was named as occluded RRM (oRRM4) (Figure 5b).⁴⁸

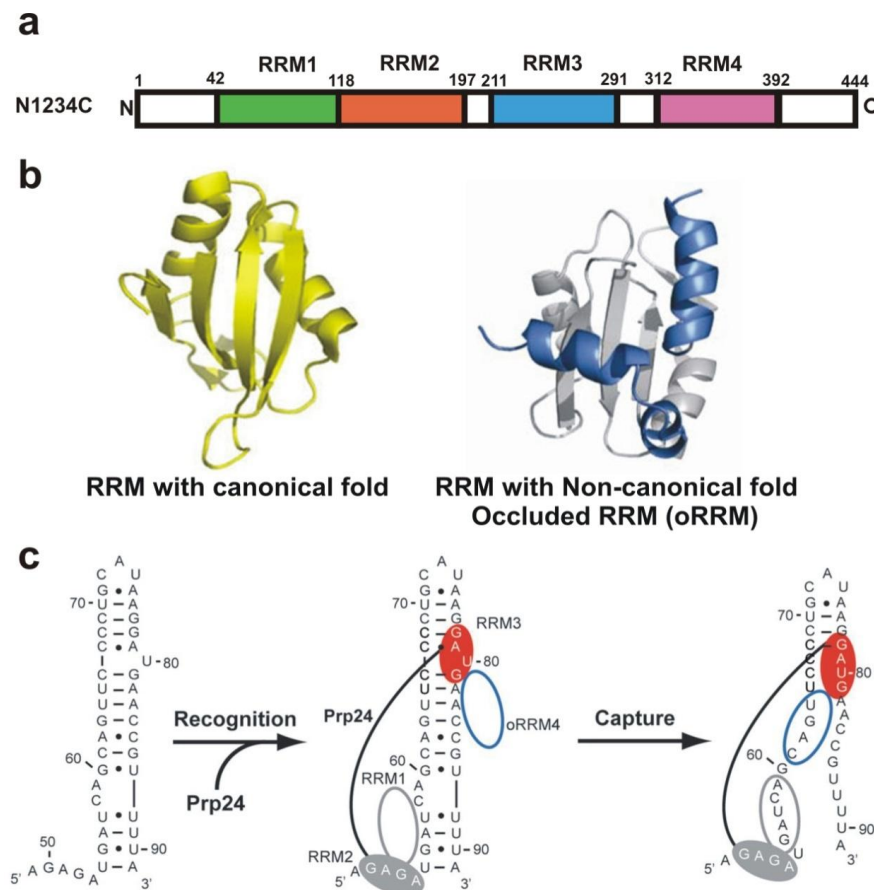


Figure 5: Prp24 acts as a U6 chaperone. (a) Schematic diagram of the four RNA recognition motifs of Prp24. (b) First three RRMs adopt a canonical fold where-as fourth the RRM folds non-canonically. (c) Schematic model showing binding of the four RRMs on different U6 regions

According to gel shift assays done by Kwan et al., RRM1 and 2 are important for high-affinity binding of Prp24 to U6, and RRM3 and 4 may have a function in controlling the stoichiometry of Prp24 binding.⁴⁹ Previous studies have shown that the high-affinity binding site for Prp24 is mainly located between the 45-87 U6 snRNA nucleotides.⁴⁹ RRM2 interacts sequence specifically with the GAGA region in the ACAGAGA loop, and RRM1 destabilizes a 3' downstream weakly paired region (nucleotides 54-61: 86-91) of U6 snRNA.^{47,48} Chemical-shift perturbation studies have suggested that RRM3 may stabilize the U6 ISL.⁴⁸ In contrast, recent studies have shown that RRM4 disrupts base pairing within the bases at the bottom of the U6 ISL.^{48,50} Unwinding of base pairs in U6 by RRM1 and 4 may allow U4 to base pair with U6, in order to form the U4/U6 complex (Figure 5c). Mutations in Prp24 that suppress the U4/U6 destabilizing mutations in U4 causing a cold-sensitive phenotype have been found within RRM3.⁴⁰ With all of these findings, it has been proposed that all four RRMs in Prp24 together induce the conformational remodeling of U6 snRNA, and the protein acts as a recycling factor during spliceosomal assembly.^{43,45} Although many studies have been done on the binding of Prp24 with U6 and its function on the formation and dissociation of U4/U6 complex, the mechanism of how it happens is still not clear.

1.5: Defects in splicing and spliceosomal components can be lethal

Proper assembly of the spliceosomal components is critical for its function, and thus defects in its assembly can be lethal.^{51,52} According to many studies done on splicing, it has been revealed that defects in the splicing reaction or in spliceosomal assembly are associated with many disease conditions such as various cancers (leukemia, ovarian cancer, etc.), neurodegenerative disorders such as Parkinson's,

genetic disorders such as Cystic fibrosis and many more.⁵³⁻⁵⁵ Studying the structural dynamics and distinct functions of snRNA complexes and the factors that affect the stability of those complexes can provide an overall idea about the structure and function of the spliceosome, which will guide us to discover novel therapeutics for splicing-related diseases.

1.6: Single-molecule FRET application for studying structural dynamics of U2-U6

Single-molecule fluorescence resonance energy transfer (sm-FRET) can be used to detect interactions between molecules and their conformational changes. Sm-FRET is a very important technique in which we can focus on one molecule at a time.^{56,57} This technique provides an idea about how individual molecules behave in a bulk solution, revealing their structural dynamics and heterogeneity in the system. Also, this is a very important tool to understand and identify transient intermediate states that cannot be revealed from bulk experiments.^{33,34,57-59}

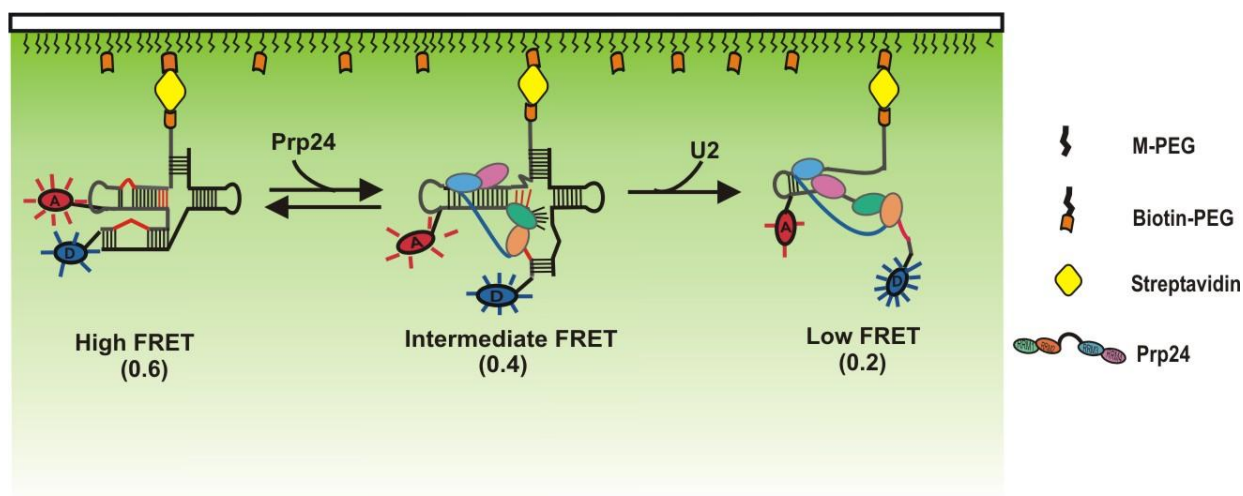


Figure 6: Single molecule experimental setup for U2/U6 complex with Prp24. The U2/U6 complex is immobilized on quartz slide via streptavidin-biotin interactions, and Prp24 is introduced separately. Donor molecules are excited by a 532 nm laser, and energy transfer from the donor to the acceptor molecules are measured and corresponding FRET values are calculated.

In our lab we use prism-based total internal reflection fluorescence (TIRF) spectroscopy. We use two fluorophore-labeled RNA constructs; cy3 as the donor and cy5 as the acceptor. A 532nm laser is used to excite the fluorophores (Figure 6).⁶⁰ An evanescent wave is created, which will only excite the molecules in the environment near the surface (~100 nm).⁶⁰ Depending on the distance between the two fluorophores, energy is transferred from the donor to the acceptor.⁶¹ The efficiency of FRET depends on the distance between the two fluorophores and is given by the Förster equation:

$$E_{FRET} = \frac{1}{1 + \left(\frac{R}{R_0}\right)^6}$$

In which R is the distance between the donor and the acceptor, R_0 is the Förster distance, which corresponds to the distance resulting in 50% efficiency of energy transfer. In our lab, the donor intensity (I_D) and acceptor intensity (I_A) of a molecule are captured by the objective, and then directed to the CCD camera as two separate channels. We then calculate the apparent FRET value using the following equation;

$$FRET = \frac{I_A}{(I_A + I_D)}$$

In which I_A is the acceptor intensity and I_D is the donor intensity. This allows us to study the variation of FRET with time, which corresponds to the conformational changes of individual molecules. The ratio of acceptor intensity to total intensity gives an idea about the distances between the fluorophores, which provides an overall picture of structural dynamics of a particular molecule. Therefore, FRET can be used as a molecular ruler to study the conformational dynamics in biological systems.^{56,62}

CHAPTER 2: Material and Methods

2.1: Sample purification and labeling

RNA samples for single-molecule experiments were purchased from the Keck Foundation Resource Laboratory at the Yale University School of Medicine. U6 was ordered with a 5'-Cy3, an internal amino C6 dT and 3' – biotin (U6; Table1). U2 was ordered with or without 3' – C7 amino linker (U2 and U2-cy5, respectively; Table 1).

Table 1: RNA sequences used in this study

Name	Modifications	Sequence (5' -3')
U6	X=dT with C6 amino linker for Cy5 labeling	Cy3-AUACAGAGAUGAUCAGCAGUUCCCCXGC AUAAGGAUGAACCGUUUUACAAAGAGAU-Biotin
U6-FI	X- Fluorescein	X-AUACAGAGAUGAUCAGCAGUUCCCCUGC AUAAGGAUGAACCGUUUUACAAAGAGAU
U2		UAUGAUGUGAACUAGAUUCGGUUUUCGGUU UCUCUA
U2-cy5	X = C7 amino linker for Cy5 labeling	UAUGAUGUGAACUAGAUUCGGUUUUCGGUU UCUCUAX

The 2'-hydroxyl protective groups were removed and the RNAs were purified as described previously.^{58,63} The RNAs were purified by denaturing gel electrophoresis (20% wt/vol polyacrylamide and 8 M urea) and diffusion elution against elution buffer (0.5 M NH₄OAc and 0.1 mM EDTA) overnight at 4 °C, followed by chloroform extraction, ethanol precipitation, and C8 reverse-phase HPLC. The C6 amino linker in U6 and C7

amino linker in U2-cy5 were labeled with Cy5 (GE Healthcare) in labeling buffer (100 mM Na₂CO₃, pH 8.5) overnight at room temperature. The labeled RNA was purified by ethanol precipitation and reverse-phase HPLC. RNA concentrations of all samples were measured by UV-Vis absorbance at 260 nm.

All the Protein samples (full length and truncated Prp24) were obtained from the Butcher's lab in University of Wisconsin-Madison. Protein samples came in the storage buffer containing 50% glycerol, 25mM Tris, 125 mM NaCl, 1.25 mM DTT and 0.2 mM EDTA.

2.2: MALDI-MS experiments

Matrix-assisted laser desorption ionization-mass spectrometry was carried out to confirm the position of the modified nucleotide used for cy5 labeling in U6 RNA as described.⁶⁴ The U6 RNA (300 pmol) were RNase T1 (~100 units) digested for 15 minutes in order to produce smaller fragments. The molecular weights of the fragments were calculated by using the Mongo Oligo Mass Calculator v2.06. After RNase T1 digestion, the reaction was stopped in dry-ice, dried and dissolved in 1ul of distilled water. 1 ul of MALDI matrix (3-hydroxypicolinic acid (HPA) in 50% acetonitrile), 0.5 µl of 100 mM ammonium citrate and 1µl of RNA sample were mixed on the MALDI plate in the given order. The spot was dried for about 30min and used in MALDI experiment. Representative spectrums for Cy3-U6 and U2-linker sample are shown in Figure 7. The fragment that appears at 2654.716 is the fragment with the modified nucleotide used for Cy5 labeling in U6. In addition to the fragment with the modified nucleotide, all the other digested fragments were also observed within a reasonable error (Table 2).

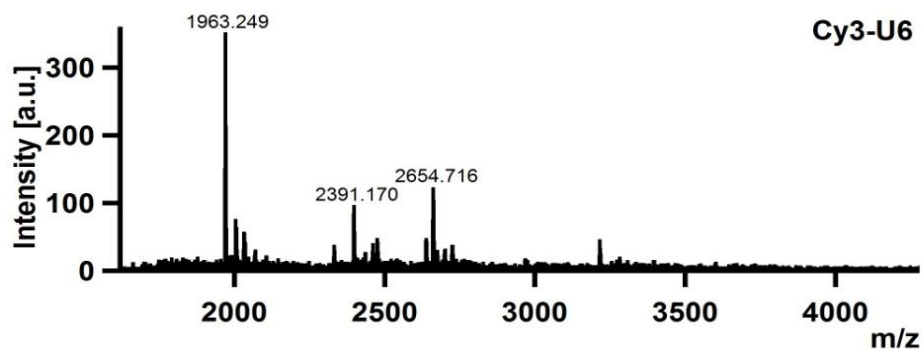


Figure 7: MALDI result reveals the mass of the fragment that is used for Cy5 labeling. The peak at 2654.716 is corresponding to the fragment containing the modified nucleotide for Cy5 labeling. The other two peaks at 1963.249 and 2391.170 are two of other fragments resulting from RNase T1 digestion.

Table 2: The expected and observed masses from MALDI-MS experiments for the RNaseT1 digested U6 RNA. All the masses are observed within a 5% error. * Not observed.

Fragment	Sequence	Expected mass	Expected mass (without 3' phosphate)	Observed mass
A1:G6	<u>pAUACAGp</u>	3267.597	3249.579	N/O*
A7:G8	<u>AGp</u>	692.433	674.418	693.985
A9:G11	<u>AUGp</u>	998.602	980.587	999.348
A12:G16	<u>AUCAGp</u>	1632.995	1614.980	1633.940
C17:G19	<u>CAGp</u>	997.617	979.602	999.348
U20:G26	<u>UUCCCCGp</u>	2654.708	2636.693	2654.716
C27:G32	<u>CAUAAGp</u>	1962.204	1944.189	1964.155
G33:G33	<u>Gp</u>	363.224	345.209	N/O*
A34:G36	<u>AUGp</u>	998.602	980.587	999.348
A37:G41	<u>AACCGp</u>	1632.010	1613.995	1633.940
U42:G51	<u>UUUUACAAAGp</u>	3209.919	3191.904	3211.360
A52:G53	<u>AGp</u>	692.433	674.418	693.985
A54:U59	<u>AUUUAU</u>	2390.739		2392.434

2.3: Fluorescence anisotropy experiments

Anisotropy experiments were carried out using a spectrofluorometer with automated polarizers (Varian, Carry Eclipse). The U6 RNA with 5' fluorescein (25 nM) and U2 RNA (50 nM) were mixed in a standard buffer (50 mM Tris-HCl, pH 7.5, 100 mM

NaCl, and 10 mM MgCl₂) and heated at 94 °C for 45 s and then annealed at room temperature for 20 min. Anisotropy was measured for Prp24 concentrations of 0 to 1 μM. Fluorescein was excited at 490 nm (5 nm bandwidth), and parallel (I_{\parallel}) and perpendicular (I_{\perp}) emission intensities were measured at 520 nm (5 nm bandwidth).

Fluorescence anisotropy (r) is given by;

$$r = \frac{I_{\parallel} - GI_{\perp}}{(I_{\parallel} + 2GI_{\perp})}$$

in which G is an empirically determined, instrument-dependent correction factor.^{65,66}

2.4: Gel-shift assays

U2/U6 complex was made by mixing U2 (4 μM)/ U6 (2 μM) or U2-cy5 (2 μM)/U6-cy3 (2 μM) in buffer (50 mM Tris-Cl, pH 7.5, 100 mM NaCl, 10 mM MgCl₂) and heating at 94 °C for 45 s, followed by 20 min incubation at room temperature for annealing. Prp24 (full length and truncated-first RRM is removed, denoted as 234C; 4 μM each) was added and incubated for ~10 min. After incubation, an equal volume of 40% glycerol was added to the reaction mixture. Non-denaturing (29:1 acrylamide:bisacrylamide ratio, 15%) gel electrophoresis was performed in 50 mM Tris-acetate, pH 7.5, 100 mM sodium acetate, 10 mM magnesium acetate, and 5 mM DTT at 4 °C for >18 hrs at 100 V. The gel was scanned using a Typhoon 9210 Variable Model Imager (GE Healthcare) and analyzed with ImageQuant software (Amersham Bioscience).

2.5: Single-molecule experiments

Single molecule experiments were performed as described.^{58, 60} Two RNA strands (2 μM U6 and 4 μM U2) in standard buffer (50 mM Tris-HCl, pH 7.4, 100 mM NaCl, and 10 mM MgCl_2) were heated at 94 °C for 45 s and annealed by cooling to room temperature over 20 min. The annealed, biotinylated, fluorophore-labeled complex was then diluted to 25 pM and immobilized on a PEGylated surface of Quartz slides via a biotin-streptavidin interaction to generate a surface density of ~ 0.1 molecules/ μm^2 . The donor fluorophores were excited in a home-built total internal reflection microscope with a laser (532 nm, 3 mW, Spectra-Physics Excelsior). The donor and acceptor emission were separated using appropriate dichroic mirrors (610DCXR, Chroma) and detected as two side-by-side images on a back-illuminated electron-multiplied CCD camera (Andor I-Xon).^{56,58,60} The individual donor (ID) and acceptor (IA) intensities were measured by integration of their relative spot intensities. The donor (ID) and acceptor (IA) fluorescence signals of optically resolved single molecules (characterized by single-step photobleaching) were detected and used to calculate the FRET ratio as $IA / (IA + ID)$, and followed in real time for each molecule.

In concentration-based experiments, the measurements were obtained under variable Protein concentrations (0 – 100 nM full length and truncated Prp24, 234C) at room temperature with an oxygen-scavenging system (OSS), consisting of 5 mM protocatechuic acid (PCA) and 0.1 μM protocatechuate 3,4-dioxygenase (PCD), to reduce photo-bleaching.⁶⁷ Resulting time trajectories were then used to draw a histogram, which represents the frequency of the population at different FRET values. A cutoff FRET value of 0.3 was used to distinguish between high and low FRET

conformations. To determine dissociation constant (K_D) values for binding of full length Prp24 and truncated proteins; the fraction of molecules with low FRET state was plotted as a function of the concentration of protein and fitted to a modified Hill equation:

$$f(\text{Prp24}) = f_0 + (f_{\max} - f_0) \frac{[\text{Prp24}]^n}{K_D^n + [\text{Prp24}]^n}$$

in which f_0 is the initial fraction of molecules at low FRET state, f_{\max} is the final fraction of molecules at low FRET state, n is the Hill coefficient, K_D is the dissociation constant and $[\text{Prp24}]$ is the concentration of protein .

In time-dependent experiments, cy3-U6 (2 μM) and U2-cy5 RNA (2 μM) strands (Figure 11a) were used and samples were prepared as described earlier. The measurements were done every five minutes and histograms were drawn for each time point. A cutoff FRET value of 0.14 was used to distinguish the FRET states corresponding to the conformations with and without U2. To determine the rate constant (K_{obs}) for dissociation of U2, the fraction of molecules with zero FRET state was plotted as a function of time and fitted to an exponential fit.

CHAPTER 3: Results and Discussion

Although many studies have revealed the role of Prp24 on U4/U6 complex, it's unclear whether it also has any role in modulating the structural dynamics of U2/U6 complex. Since it was suggested that Prp24 acts as a recycling factor and is also tightly associated with U6, we propose that Prp24 may be involved in unwinding the U2/U6 complex after catalysis, and therefore helping to recycle snRNAs. To study the effect of Prp24 on the structural dynamics of U2/U6 complex and the role of Prp24 as a chaperone to unwind U2 from the complex, we carried out single-molecule FRET experiments in the presence and absence of full length and truncated Prp24. Doing sm-FRET allows us to determine the actual K_D for Prp24 binding, structural dynamics of the complex and the intermediate steps occur during unwinding of the U2.

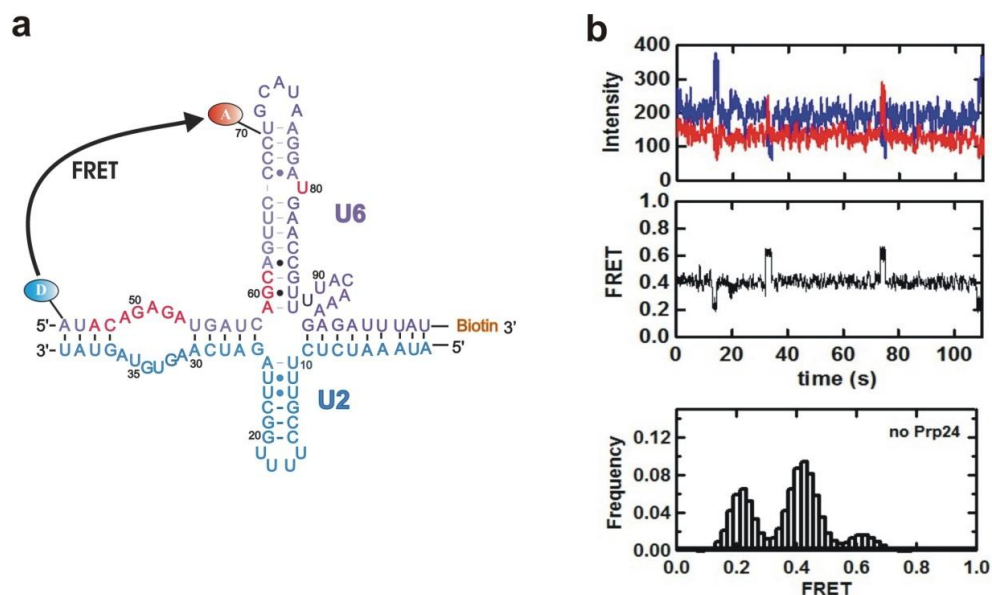


Figure 8: Structural dynamics of the U2/U6 complex in the absence of Prp24 **(a)** Secondary structure model of the spliceosomal snRNAs U2-U6 of *Saccharomyces cerevisiae*. U6 strand (purple) is labeled with cy3 at the 5' end, internal cy5 and biotin at the 3' end. U2 (blue) base paired with U6. Highly conserved residues are highlighted in red. **(b)** Time trajectory of a single U2/U6 complex (10 mM Mg^{2+}). Top: individual donor (blue) and acceptor (red) intensities and resulting FRET trajectory. Bottom: corresponding FRET histogram. Three distinct FRET states indicate the presence of three conformations.

We used the minimal U6 strand (nucleotide 45-104) including the GNRA pentaloop and minimal U2 strand, to study the effect of Prp24 on the dynamics of U2/U6 complex using sm-FRET (figure 8a). The labeling strategy is similar to previous study, and RNAs were purified, labeled and immobilized on quartz slides (figure 6) as described in the Material and Methods section.

3.1: Gel-shift assay and fluorescence-anisotropy measurements reveal binding of Prp24 with the yeast minimal U2/U6 construct

Previous studies on Ppr24 have shown that Prp24 binds to U6 tightly and only associates with U6, but not with U4. Apparent K_D values for binding of full-length and truncated (some RRM1s were removed) Prp24 were observed previously using gel-shift assays and filter-binding assays.⁴⁹ Similarly, we have carried out gel-mobility-shift assays and fluorescence-anisotropy experiments to check binding of Prp24 to the minimal U2/U6 complex used in this study.

We incubated preformed U2/U6 complex with full length Prp24 or truncated protein, (RRM1 removed; denoted as 234C), and ran a native gel (Figure 9a). Lane 1 of the figure 9a has only U6, represents by the high intensity band. The low intensity band migrating slower than the main band in the lane 1 may correspond to randomly folded U6, given that we were not been able to see that band in a denaturing gel. The shift in the band at second lane corresponds to formation of the U2/U6 complex. The slower migrating band in 3rd lane corresponds to Prp24 bound to U2/U6 complex. Interestingly, the Prp24-U2/U6 complex shows lower FRET than the U2/U6 complex alone, suggesting that binding of Prp24 induces a rearrangement in the U2/U6 complex,

resulting in a low FRET conformation. The 4th lane has a very faint band that corresponds for the Prp24-U2/U6 complex, suggesting that the binding of truncated protein, 234C, is few folds less than that of full-length protein. This result is in good agreement with the gel-shift results of the Brow lab, in which deletion of RRM1 leads to five-fold decrease in the Prp24 binding affinity for U6.⁴⁹ In the 3rd and 4th lanes, some of the sample has retained, may be due to the formation of higher order complexes with U2/U6 and Prp24 result in the bright bands.

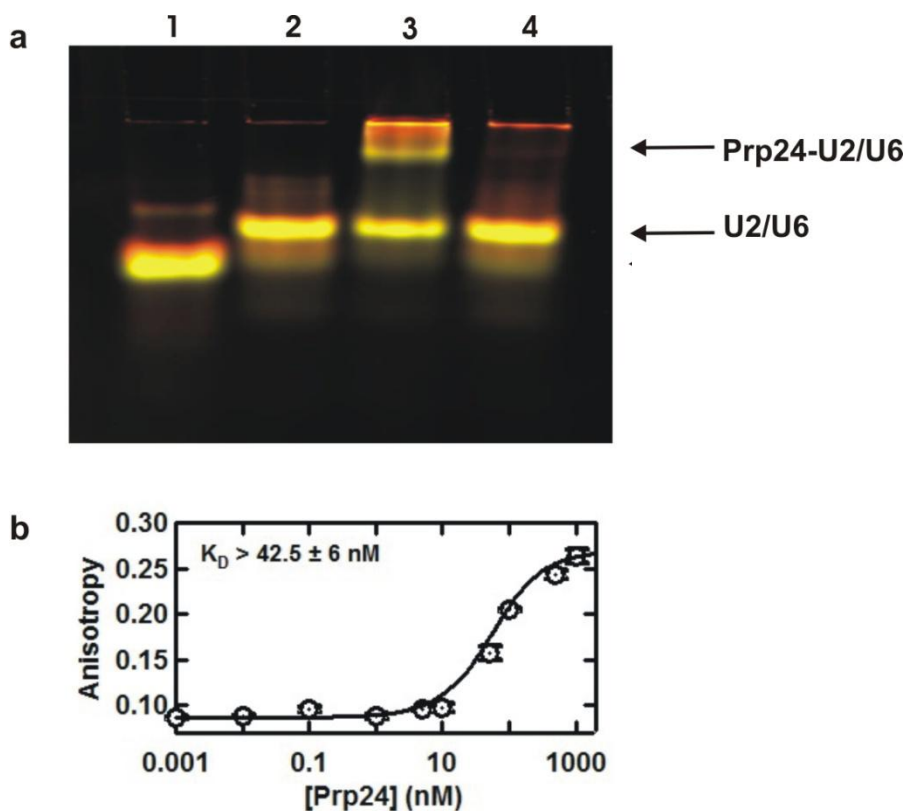


Figure 9: Prp24 binds to U2/U6 complex. (a) Gel-shift assay with Prp24 and the U2/U6 complex. Lane 1: U6 only, Lane 2: U2/U6 complex, Lane 3: U2/U6 with Prp24, Lane 4: U2/U6 with 234C. (b) Fluorescence anisotropy experiment with U2/U6 complex at different Prp24 concentrations. Anisotropy data was plotted against Prp24 concentration and fitted to a quadratic binding equation.

To further characterize binding of Prp24 to the U2/U6 complex, we performed fluorescence anisotropy experiments. In anisotropy, the fluorophores attached to a particular molecule are excited using polarized light. The excitation of the fluorophores depends on the orientation of those against the applied polarization. If the fluorophores are not changing their orientation, the emission light also is polarized. Freely moving fluorophores show a reduction in the polarization of the emitting light. On the other hand if the fluorophore cannot rotate freely the emitting polarization will be high.^{65,66} This phenomenon is used in fluorescence anisotropy experiments to check the protein-RNA interactions. We attached Fluorescein to U6 RNA (U6-fl) and anneal the complex with unlabeled U2. In the absence of Protein, fluorophore attached to the U6 snRNA rotates in a characteristic time scale which will then result in a relatively low anisotropy value. Upon Prp24 binding to U2/U6 complex, the movement of RNA (and therefore its attached fluorophore), will be hindered and the anisotropy will increase. The change in anisotropy is proportional to the fraction of U2/U6 complex bound to Prp24. By measuring the fluorescence anisotropy at different Prp24 concentrations and fixing data in to quadratic equation, we were able to estimate the dissociation constant for Prp24 binding to the U2/U6 complex.

$$f(\text{Prp24}) = r_0 + (r_{\max} - r_0) \left[\frac{K_D + [\text{RNA}_0] + [\text{Prp24}] - \sqrt{(K_D + [\text{RNA}_0] + [\text{Prp24}])^2 - 4[\text{RNA}_0][\text{Prp24}]}}{(2 * \text{RNA}_0)} \right]$$

In the equation above, r_0 is lowest anisotropy value, r_{\max} is highest anisotropy value, $[\text{Prp24}]$ is the corresponding protein concentration, $[\text{RNA}]$ is the concentration of

U6-fl used and K_D is the dissociation constant. Since, in the fluorescence-anisotropy experiments RNA concentration is limited (we have to use at least 25nM fluorescein-labeled RNA), the fit in figure 9b yielded an apparent K_D value, but not the actual. The apparent K_D value for the Prp24-U2/U6 complex obtained by this experiment is 42 ± 6 nM. Previous gel-shift results of the Brow lab⁴⁹ has come up with an apparent K_D value of 43 ± 11 nM, and our K_D value is similar to that.

3.2: Presence of Prp24 affects the structural dynamics of U2/U6 complex

According to our hypothesis, if binding of Prp24 induces a conformational change in the U2/U6 complex, we should obtain different FRET states distributions in the presence and absence of Prp24. Previous studies carried out in our lab using minimal U2 and minimal U6 RNAs suggested that the U2/U6 complex adopts at least three distinct conformations corresponding to three different FRET states.³³ Figure 8b represents a typical FRET trajectory, and the corresponding histogram obtained for the U2/U6 complex at 10 mM Mg^{2+} which clearly shows three FRET values corresponding to three distinct conformations, which is in accordance with the previous single molecule data.³³ A characteristic FRET trajectory and FRET histogram in the presence of Prp24 are shown in Figure 10a. Addition of Prp24 resulted in static 0.2 FRET state compare to the dynamic three FRET states in the absence of Prp24. The FRET histogram show, in the presence of Prp24, there is a dramatic increase of the 0.2 FRET population, indicating that the binding of Prp24 with U2/U6 complex affects the structural dynamics of U2/U6 complex.

In order to confirm the specificity of Prp24 at stabilizing the low FRET state, we carried out similar single-molecule FRET experiments with PTB (polypyrimidine tract binding) protein and Mss116 at 100 nM concentrations. PTB protein is a RNA binding protein with RNA recognition motifs similar to the Prp24.³⁵ PTB has used as a control in this experiment, due to its similarities. If the resulting change in the FRET states is due to a binding of RNA binding protein and it has a better chance that binding of PTB also giving a same result. Similarly, Mss116, an ATP-dependent RNA helicase⁶⁸, should make such change in the FRET states by its helicase activity. Histograms in figure 10b show that there is no increase in the 0.2 FRET state at a higher concentration of both PTB and Mss116, revealing that the inducing conformational changes in U2/U6 complex and stabilizing low FRET state are specific for Prp24.

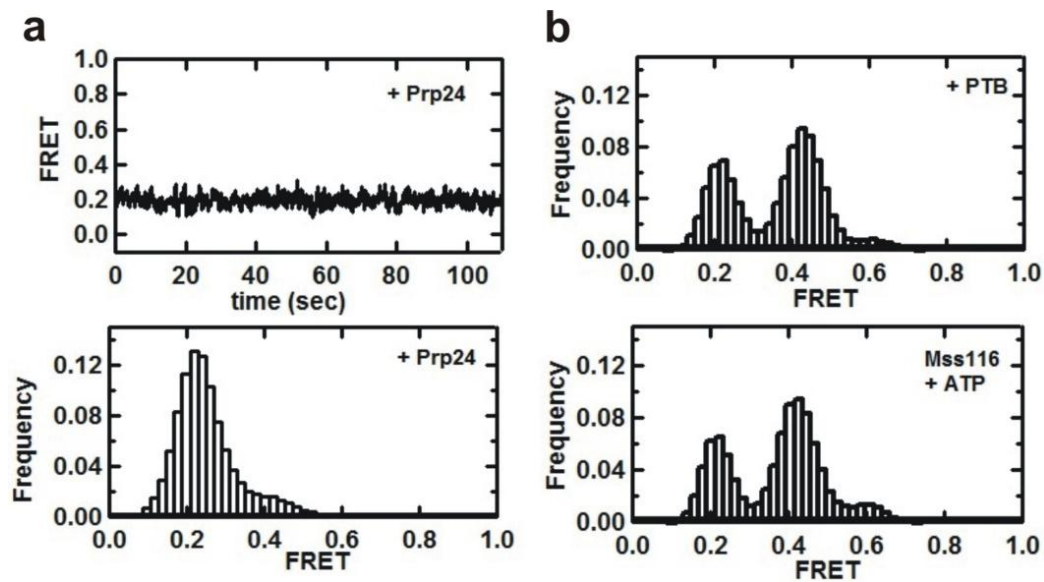


Figure 10: Binding of Prp24 with the U2/U6 complex stabilizes the low FRET conformation. **(a)** The single-molecule FRET time trajectory and the corresponding histogram in the presence of Prp24. Prp24 shifts the FRET ratio to 0.2, revealing a conformational change in the U2/U6 complex. **(b)** Histograms for the control single-molecule experiments with PTB and Mss116 proteins reveal that conformational change in U2/U6 is specific for Prp24.

3.3: Effect of RRM1 on the binding of Prp24 with U2/U6 complex

As stated in previous studies, the four RRM1s of Prp24 have different functions in formation and destabilization of the U4/U6 complex. Among the four RRM1s, it has been shown that RRM1 is more important for the high affinity binding of Prp24 to U6.⁴⁹ To study the effect of RRM1 on the binding of Prp24 with U2/U6 complex, we carried out a set of single-molecule experiments at various concentrations of the full-length protein (Prp24) and truncated protein (234C), where the N-terminus and RRM1 have been removed⁴⁹. For this set of experiments, we kept $[Mg^{2+}]$ constant at 10 mM. In the presence of the full length protein (Prp24), histograms were built for each Prp24 concentration. Then, we divided the integral of the peak at 0.2 FRET by the total integral of all the peaks, obtaining the fractions of molecules at 0.2 FRET for each Prp24 concentration (Figure 11a). Those fraction values were plotted as a function of Prp24 concentration and fitted to the modified Hill equation. As shown in figure 11a, in the absence of Prp24, more molecules tend to be in higher FRET states (0.4 and 0.6). Upon increasing Prp24 concentration, the fraction at 0.2 FRET state increases, reaching a plateau at Prp24 concentrations above 5 nM. The titration curve (Figure 11b), yields a K_D value of ~2 nM, indicating a tight binding of Prp24 to U6. Since in single-molecule FRET experiments we immobilize the RNA, the RNA concentration is considered as zero and thus the resulting K_D value has not limited by the RNA concentration, which will be the actual K_D value for the Prp24 binding. According to the previous gel-shift results of Brow lab, the actual K_D value for the full-length Prp24 is ~ 2 nM, which has calculated from bulk binding studies. Our data has given a ~10 fold lower

K_D . The difference between two K_D values may be due to the use of single-molecule experiments, where we consider one molecule at a time.

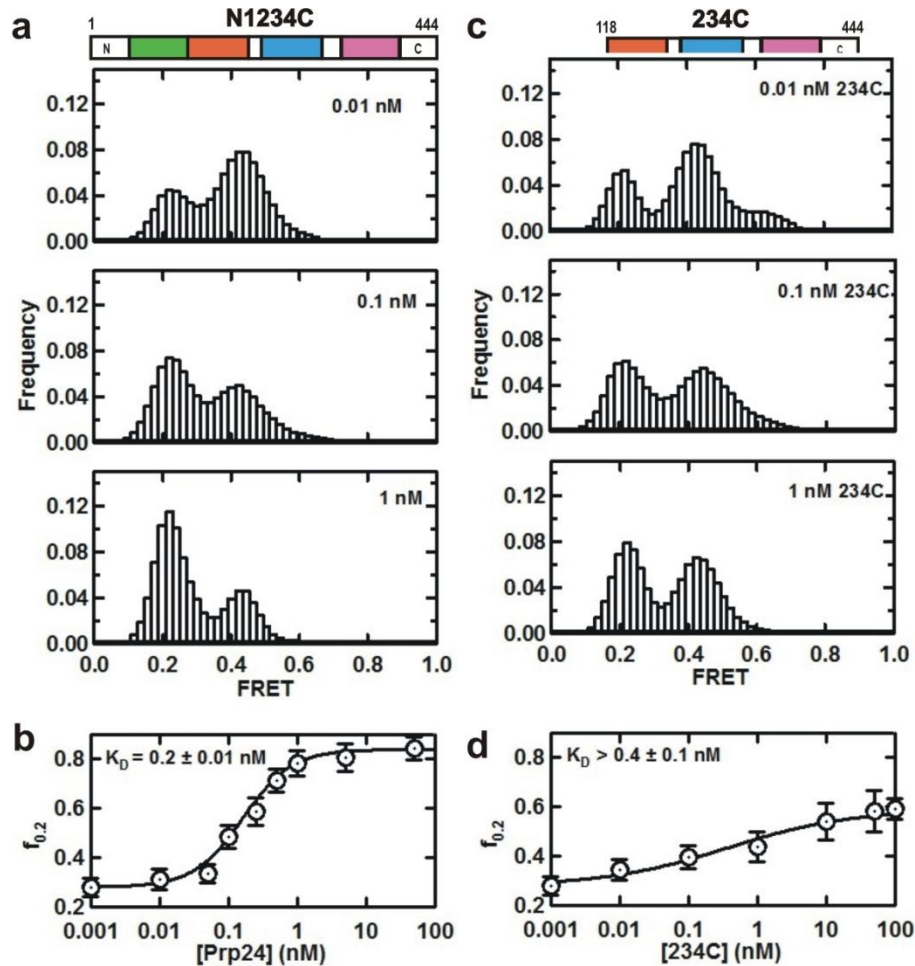


Figure 11: of full-length Prp24 (a) and truncated 234C (c) on the conformational dynamics of U2/U6. Each panel corresponds to an average smFRET histogram from >100 single-molecule trajectories at the indicated full-length and truncated protein concentrations. The fraction of molecules in the 0.2 FRET state is plotted against Prp24 (b) and 234C (d) concentrations and fitted to a Langmuir equation to yield the K_D values for the binding of protein to U2/U6 complex.

In order to characterize the role of RRM1 in binding and activity, we carried out another set of experiments with different concentrations of 234C, the truncated protein in which RRM1 has removed. All the experiments and analysis were done in the same

way as explained above for the full-length protein. When RRM1 is removed, only ~58% of molecules found to be in 0.2 state, whereas ~42% are in 0.4 state (figure 11c). This indicates that RRM1 is important for Prp24 binding to U2/U6 complex. The lower affinity of 234C allows U2/U6 to undergo dynamics to some extent, which results in 40% of the molecules having a 0.4 FRET state. Despite the decrease in binding upon RRM1 removal, a stabilization of the 0.2 FRET state could be observed, indicating that the rest of the protein can bind to U2/U6 complex and stabilize the low FRET conformation. Previous studies have shown that RRM1 interacts with the phosphate backbone of 3' downstream GAUCA sequence via electrostatic interactions and when RRM1 is removed, binding affinity of Prp24 is reduced.⁴⁹ Gel shift binding assays demonstrated that RRM1 and RRM2 are important for the high affinity binding of U6 snRNA and removal of RRM1 results in a five-fold reduction in the binding of Prp24.⁴⁹ Although our gel-shift assay have also revealed similar results where 234C shows few fold lower binding with U2/U6 complex resulting a very low intensity band in the gel, our single-molecule results have not shown such a big different between the effect from full-length and 234C protein. According to the single-molecule data, only about 60% of the molecules stay at 0.2 FRET state in the presence of 234C, whereas about 80% of molecules stay at 0.2 FRET state in the presence of full-length protein. Calculated K_D for the 234C binding is ~0.4nM, which is just a two fold increase than that of full-length protein (Figure 11d). This suggests that the higher concentrations of 234C also facilitate the conformational dynamics of U2/U6, but it is less effective than the full-length protein. Therefore we suggest that with removal of RRM1, the magnitude of disruption of base

pairing between U2 and U6 may be reduced and the low FRET conformation is less stabilized.

These results can be explained according to the previously proposed model for binding of different RRM1s to U6.^{48,49} RRM1 binds with the 3' downstream GAUCA bases, which are involved in base pairing with U2 in the U2/U6 complex. Binding of Prp24 with the U2/U6 complex can destabilize those base pairings, resulting in a disruption of helix I. In addition, RRM4 disrupts the lower region of U6 ISL.⁴⁸ Altogether, these disruptions will result in the formation of a large bulge consisting of ACAGAGA loop, downstream GAUGA sequence, and the bases in the lower ISL region, which might weaken the base-pairing in helix III. These changes in U2/U6 may cause a conformational change that result in a low FRET state. When RRM1 is removed, disruption of base pairing at helix I is prevented. Therefore, the effect of formation of the extended loop is reduced, leading to a concomitant reduction in the magnitude of the disruption of base pairing between U2 and U6. The difference between our K_D and the previously published data can again be due to the use of single-molecule experiments, which provides actual K_D values because it doesn't limit the RNA concentration as in the bulk studies. This model explains why the 0.2 FRET state is less populated, even at a higher [234C] and why it shows a lesser effect on the conformational dynamics of U2/U6 compared to full-length protein.

3.4: Binding of Prp24 facilitates the unwinding of U2 from the complex

Previous studies have shown that Prp24 acts as a chaperone and binding of Prp24 can disrupt the base pairings, resulting in a destabilization of the U6 ISL. Similarly, our single-molecule data also revealed that binding of Prp24 induces a conformational change in U2/U6, and thus, we suggest that it occurs via disruption of base pairing between U2 and U6, especially within helix I and III. To test whether Prp24 acts as a chaperone and facilitates the unwinding of U2 from the complex, we have done a gel-shift assay followed by single-molecule experiments with a different labeling pattern. For this set of experiments we labeled the 3' end of U2 with cy5 using a C7 amino linker, and used 5' -cy3 labeled and 3' biotin attached U6 (Figure 12a). According to the position of the fluorophores, if the U2/U6 complex is formed, we should get high FRET. On the other hand, if binding of Prp24 destabilizes base pairing between U2 and U6 and unwinds U2 from U6 as suggested earlier, we should then obtain a zero or a low FRET value. Using this construct, we carried out experiments to determine the effect of Prp24 and 234C in the unwinding of U2 from the complex.

First we have done a gel-shift assay as described in Materials and Methods. Lane 1 and 2 of figure 12b correspond to U2 and U6 RNA strands alone and the clear shift in lane 3 is indicating the formation of U2/U6 complex. The color of the band represents the corresponding FRET of the complex, which confirms the adoption of a high FRET conformation by the U2/U6 complex. The larger shift in lane 4 corresponds to the binding of Prp24 with the complex, and green color of the band suggests that the Prp24-U2/U6 complex is adopting a low FRET conformation. This is in accordance with our previous results (3.2, 3.3) in which binding of Prp24 stabilizes a low FRET conformation.

Increase of free U2 in the presence of Prp24 confirms our hypothesis that binding of Prp24 disrupts the base pairing between U2 and U6 and results in unwinding of U2 from the complex. The slow migrating green band in the presence of Prp24 may be due to the formation of a low FRET conformation of U6 as a result of removal of the U2 strand from the complex.

To confirm the unwinding of U2 in the presence of Prp24, we carried out single-molecule flow experiments, in which we flow Prp24 in standard buffer solution in real time. The results of this experiment show a change of FRET from 1 to zero upon introducing Prp24 in solution via an intermediate state of 0.2 (Figure 12c). We have done a control experiment where we flow the buffer without Prp24 (Figure 12d). The resulting traces barely showed any change in FRET state before and after the flow, confirming that the FRET change occurs due to the binding of Prp24.

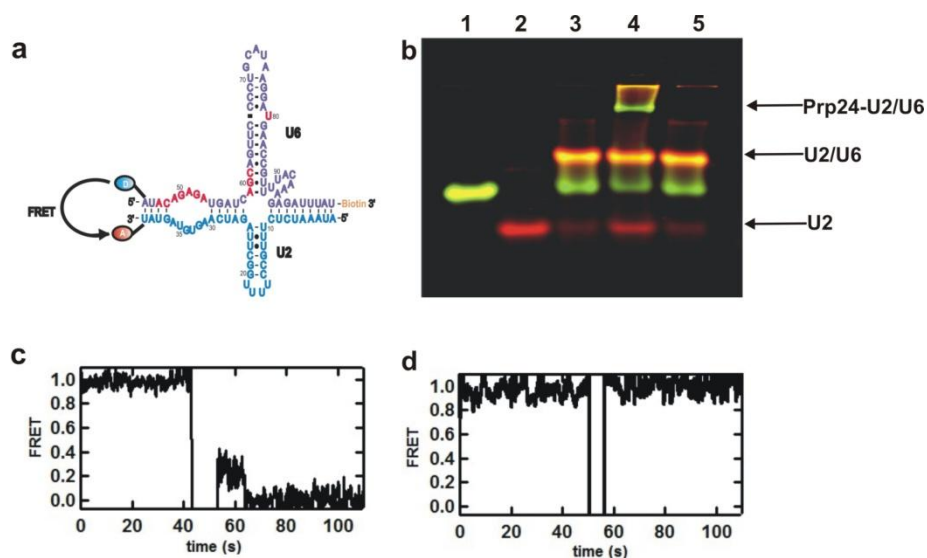


Figure 12: Prp24 induces unwinding of U2 from the complex. (a) Schematic diagram of U2/U6 complex used. Cy3 (donor) is attached to U6 and cy5 (acceptor) is attached to U2. (b) Gel-shift assay with U2/U6 complex and Prp24. Lane 1: cy3-U6, Lane 2: U2-cy5, Lane 3: U2/U6 complex, Lane 4: U2/U6 with Prp24, Lane 5: U2/U6 with 234C. (c) and (d) Characteristic FRET trajectories for single-molecule flow experiment with (c) and without (d) Prp24.

Then, we carried out single-molecule time-dependent experiments (as described in Materials and Methods section), to confirm that the formation of zero FRET state is not due to photobleaching of cy5, but unwinding of U2 from the complex upon Prp24 binding. We have done these experiments at different concentrations of Prp24 and 234C and as a control we did experiments with buffer only (Figure 13a). Upon addition of Prp24, the zero FRET population increased over time. In order to get the true rate for the U2 removal we first deduct the fraction of molecules at zero FRET due to photobleaching of fluorophores at each time point and then the resulting data were fitted to a mono-exponential function, yielding a rate (k_{obs}) of $\sim 0.15 \text{ min}^{-1}$ in the presence of Prp24 (Figure 13b). Then we calculated the maximum fraction of molecules at zero FRET at different Prp24 concentrations and again did the correction for photobleaching. These data were then fitted to the modified hill equation and obtained dissociation constant (K_D) of $\sim 0.3 \text{ nM}$ (Figure 13c). In contrast when 234C is added, rate of U2 removal has reduced by \sim four fold ($k_{\text{obs}} \sim 0.8 \text{ min}^{-1}$) and the dissociation constant has reduced by \sim ten fold ($K_D \sim 3.0 \text{ nM}$) (Figure 13b and c). These results indicate that binding of Prp24 has destabilized the base pairing between U2 and U6 resulting a removal of U2 from the complex. The removal of U2 from the complex has increased over time and in the presence of higher Prp24 concentrations. On the other hand the binding affinity of prp24 to U6 has reduced when RRM1 is removed and thus it reduced the rate of removal of U2 from the complex.

With these data we proposed a model for the role of Prp24 in the removal of U2 from minimal U2/U6 complex. Binding of Prp24 with the minimal U2/U6 complex can disrupts the base pairing between U2 and U6 in helix I, as well as in the lower region of

U6 ISL resulting in low FRET (0.2 or zero). Furthermore, the destabilization of helix I and lower region of ISL may result in the formation of an extended loop, accompanied by the disruption of four base pairs at the helix III. These sequential events will lead to a destabilization of helix II, facilitating the removal of U2 (Figure 14). On the other hand, when RRM1 was removed, we observed ~ 5-10 fold reduction in the formation of low (Figure 10a,c) or zero (Fig.13a) FRET conformations compared to that of full-length protein, which suggested that the truncated protein, 234C cannot bind to the U2/U6 complex as tight as full-length protein and thus it cannot destabilizes the base pairing as efficient as full-length protein. Therefore it results in a lower rate and a lower dissociation constant than that of full-length protein.

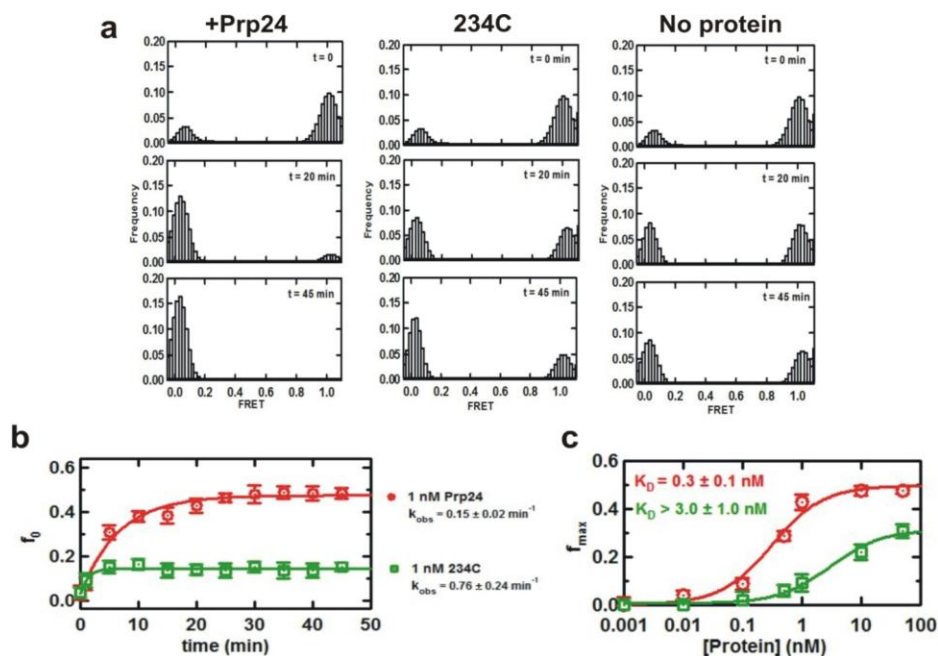


Figure 13: Binding of Prp24 facilitates the removal of U2. **(a)** Histograms from single molecule time dependent experiments for Prp24 (left), 234C (middle) and control (right), showing the change in zero FRET state along with the time. **(b)** Fraction of molecules at zero FRET as a function of time was plotted to obtain the rate of removal of U2 in the presence of Prp24 (red) and 234C (green). **(c)** Fraction of molecules at zero FRET as a function of Prp24 concentration (red) and 234C concentration (green) was plotted to obtain the dissociation constant for U2 removal. In both (b) and (c), photobleaching rate has removed.

In summary in the light of the results we obtained, we suggest that Prp24 plays an important role in U2 and U6 snRNP recycling by dissociating the U2/U6 complex. Due to the short lengths of minimal U2/U6 complex, binding of Prp24 results in a complete dissociation of two snRNAs from each other. Although we found that the Prp24 facilitates the complete removal of U2 from the minimal U2/U6 complex, we suggest there may be other protein factors such as some helicases are also involved in this process at cellular level, where full-length U2 and U6 snRNAs are present. After U2 dissociates, Prp24 may remain bound to the U6 and also stabilizes U6 in an intermediate conformation, preventing the premature activation of U6 and later it binds with U4 to form the U4/U6 complex and join with another spliceosomal assembly cycle.

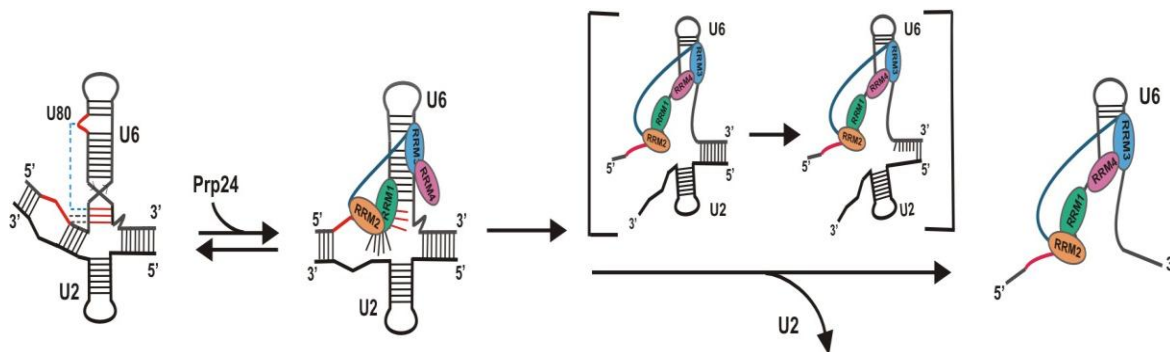


Figure 14: The proposed model for the role of Prp24 on the conformational dynamics of U2/U6 complex. In the presence of Prp24, base pairing between U2 and U6 RNAs are disrupted and U2 is unwound from U6, suggesting a novel role for Prp24 in recycling spliceosomal snRNAs.

CHAPTER 4: Conclusions and future directions

The spliceosome is a large RNA-protein complex that catalyses the splicing reaction, in which introns are removed and exons are religated to form mature mRNA. The spliceosome consists of five snRNPs and numerous proteins. Assembly of these snRNPs and proteins at different steps is crucial for its function. Some of the proteins are involved in assembly and catalysis, some are ATP-dependent helicases, and some are ATP-independent RNA chaperones, which facilitates the structural rearrangements of snRNA complexes in spliceosome. One of these proteins is Prp24, a U6-associated chaperone. Previous studies have shown that Prp24 is important for formation of the U4/U6 complex, and some studies have suggested that it may also be involved in the dissociation of U4/U6 prior to the formation of U2/U6 complex, which is the catalytically active complex^{42,44,64}. These studies proposed that Prp24 acts as a recycling factor helping to unwind U4/U6, and it helps them to form a complex again at a later stage of the spliceosomal assembly pathway. Also, some studies suggested that after removing U4, Prp24 stays bound to U6 and prevents premature formation of the active conformation. Therefore, Prp24 seems to play an important role in spliceosomal assembly^{41,44}.

We have carried out single-molecule experiments to study the effect of Prp24 on the conformational dynamics of minimal U2/U6 complex. According to our previous studies, in the absence of Prp24, U2/U6 complex shows three distinct FRET states corresponding to three conformations. During our first set of experiments using doubly labeled U6 and unlabeled U2, we observed that addition of Prp24 stabilizes the low FRET (0.2) conformation. In contrast, the truncated protein, 234C in which the first RRM

was removed, is less efficient in promoting formation of the low FRET conformation. As proposed in previous studies, RRM1 is important for the high-affinity binding of Prp24 with U6⁴⁹. Therefore, removal of RRM1 weakens binding, resulting in a less efficient stabilization of the low FRET state even at high concentrations of 234C. To test if Prp24 plays a role in unwinding U2 from the complex, we used a construct with a cy3 label on U6 and a cy5 label on U2. Data from these experiments shows that upon addition of Prp24, the zero FRET state becomes populated over time, whereas when 234C is added, increase in the zero FRET state with time is ~four fold lesser over time. Also, gel shift assays with this construct shows that addition of Prp24 increases the level of free U2, suggesting that binding of Prp24 facilitates the removal of U2 from the complex.

After two catalytic reactions and formation of mature mRNA, snRNAs should dissociate from each other to start a new cycle of spliceosome assembly. Previous studies have proposed that the ATP-dependent, DExD/H-box family protein Prp43 is involved in releasing U2, U5 and U6 after the completion of catalysis⁶⁹. Similar to Prp24, Brr2; another DExD/H-box family protein, is also involved in unwinding the U4/U6 complex⁷⁰. In light of our results, we propose⁷⁰ that Prp24 helps to unwind the minimal U2/U6 complex of yeast, similar to its function in dissociation of U4/U6. However in cellular conditions, in which full-length U2/U6 is associated with U5 at the catalytic core, other than Prp24, Prp43 may also involve in the unwinding of U2 from U6, and also destabilizing U5 from U2 and U6 snRNAs, which results in dissociation of all three snRNAs from each other. With all these findings, we propose that Prp24 plays an important role in U2 and U6 snRNP recycling by dissociating the U2/U6 complex.

To further investigate the role of Prp24 and specific binding sites of RRMs, we propose to use fluorescently labeled Prp24 in single-molecule experiments. With these results we will be able to determine how each RRM contributes on the overall function of Prp24. We also plan on doing single-molecule experiments under cellular conditions with spliceosomal extracts, which will help us to understand the role of Prp24 and Prp43 together in releasing U2, U5 and U6 after completion of catalytic reactions. These future studies will help us to reveal how Prp24 acts as a recycling factor helping to unwind U2 from the active complex.

REFERENCES

1. Wahl, M.C., Will, C.L. & Luhrmann, R. The spliceosome: design principles of a dynamic RNP machine. *Cell* **136**, 701-18 (2009).
2. Will, C.L. & Luhrmann, R. Spliceosome structure and function. *Cold Spring Harb Perspect Biol* **3**(2011).
3. Valadkhan, S. snRNAs as the catalysts of pre-mRNA splicing. *Curr Opin Chem Biol* **9**, 603-8 (2005).
4. Warf, M.B. & Berglund, J.A. Role of RNA structure in regulating pre-mRNA splicing. *Trends Biochem Sci* **35**, 169-78 (2010).
5. Black, D.L. Mechanisms of alternative pre-messenger RNA splicing. *Annu Rev Biochem* **72**, 291-336 (2003).
6. Saltzman, A.L., Pan, Q. & Blencowe, B.J. Regulation of alternative splicing by the core spliceosomal machinery. *Genes Dev* **25**, 373-84 (2011).
7. Dunn, E.A. & Rader, S.D. Secondary structure of U6 small nuclear RNA: implications for spliceosome assembly. *Biochem Soc Trans* **38**, 1099-104 (2010).
8. Ritchie, D.B., Schellenberg, M.J. & MacMillan, A.M. Spliceosome structure: piece by piece. *Biochim Biophys Acta* **1789**, 624-33 (2009).
9. Will, C.L. & Luhrmann, R. Splicing of a rare class of introns by the U12-dependent spliceosome. *Biol Chem* **386**, 713-24 (2005).
10. Schultz, A., Nottrott, S., Hartmuth, K. & Luhrmann, R. RNA structural requirements for the association of the spliceosomal hPrp31 protein with the U4 and U4atac small nuclear ribonucleoproteins. *J Biol Chem* **281**, 28278-86 (2006).

11. Lin, C.F., Mount, S.M., Jarmolowski, A. & Makalowski, W. Evolutionary dynamics of U12-type spliceosomal introns. *BMC Evol Biol* **10**, 47 (2010).
12. Valadkhan, S. & Jaladat, Y. The spliceosomal proteome: at the heart of the largest cellular ribonucleoprotein machine. *Proteomics* **10**, 4128-41 (2010).
13. Warkocki, Z. et al. Reconstitution of both steps of *Saccharomyces cerevisiae* splicing with purified spliceosomal components. *Nat Struct Mol Biol* **16**, 1237-43 (2009).
14. Makarov, E.M. et al. Small nuclear ribonucleoprotein remodeling during catalytic activation of the spliceosome. *Science* **298**, 2205-8 (2002).
15. O'Keefe, R.T., Norman, C. & Newman, A.J. The invariant U5 snRNA loop 1 sequence is dispensable for the first catalytic step of pre-mRNA splicing in yeast. *Cell* **86**, 679-89 (1996).
16. Segault, V. et al. Conserved loop I of U5 small nuclear RNA is dispensable for both catalytic steps of pre-mRNA splicing in HeLa nuclear extracts. *Mol Cell Biol* **19**, 2782-90 (1999).
17. Valadkhan, S., Mohammadi, A., Jaladat, Y. & Geisler, S. Protein-free small nuclear RNAs catalyze a two-step splicing reaction. *Proc Natl Acad Sci U S A* **106**, 11901-6 (2009).
18. Mefford, M.A. & Staley, J.P. Evidence that U2/U6 helix I promotes both catalytic steps of pre-mRNA splicing and rearranges in between these steps. *RNA* **15**, 1386-97 (2009).
19. Jacquier, A. Self-splicing group II and nuclear pre-mRNA introns: how similar are they? *Trends Biochem Sci* **15**, 351-4 (1990).

20. Keating, K.S., Toor, N., Perlman, P.S. & Pyle, A.M. A structural analysis of the group II intron active site and implications for the spliceosome. *RNA* **16**, 1-9 (2010).
21. Konforti, B.B. et al. Ribozyme catalysis from the major groove of group II intron domain 5. *Mol Cell* **1**, 433-41 (1998).
22. Huppler, A., Nikstad, L.J., Allmann, A.M., Brow, D.A. & Butcher, S.E. Metal binding and base ionization in the U6 RNA intramolecular stem-loop structure. *Nat Struct Biol* **9**, 431-5 (2002).
23. Wolff, T. & Bindereif, A. Conformational changes of U6 RNA during the spliceosome cycle: an intramolecular helix is essential both for initiating the U4-U6 interaction and for the first step of slicing. *Genes Dev* **7**, 1377-89 (1993).
24. Madhani, H.D., Bordonne, R. & Guthrie, C. Multiple roles for U6 snRNA in the splicing pathway. *Genes Dev* **4**, 2264-77 (1990).
25. Sashital, D.G., Cornilescu, G., McManus, C.J., Brow, D.A. & Butcher, S.E. U2-U6 RNA folding reveals a group II intron-like domain and a four-helix junction. *Nat Struct Mol Biol* **11**, 1237-42 (2004).
26. Rhode, B.M., Hartmuth, K., Westhof, E. & Luhrmann, R. Proximity of conserved U6 and U2 snRNA elements to the 5' splice site region in activated spliceosomes. *EMBO J* **25**, 2475-86 (2006).
27. Madhani, H.D. & Guthrie, C. Dynamic RNA-RNA interactions in the spliceosome. *Annu Rev Genet* **28**, 1-26 (1994).
28. Staley, J.P. & Guthrie, C. Mechanical devices of the spliceosome: motors, clocks, springs, and things. *Cell* **92**, 315-26 (1998).

29. Newman, A.J. & Norman, C. U5 snRNA interacts with exon sequences at 5' and 3' splice sites. *Cell* **68**, 743-54 (1992).
30. Madhani, H.D. & Guthrie, C. A novel base-pairing interaction between U2 and U6 snRNAs suggests a mechanism for the catalytic activation of the spliceosome. *Cell* **71**, 803-17 (1992).
31. Burke, J.E., Sashital, D.G., Zuo, X., Wang, Y.X. & Butcher, S.E. Structure of the yeast U2/U6 snRNA complex. *RNA* **18**, 673-83 (2012).
32. Sun, J.S. & Manley, J.L. A novel U2-U6 snRNA structure is necessary for mammalian mRNA splicing. *Genes Dev* **9**, 843-54 (1995).
33. Guo, Z., Karunatilaka, K.S. & Rueda, D. Single-molecule analysis of protein-free U2-U6 snRNAs. *Nat Struct Mol Biol* **16**, 1154-9 (2009).
34. Guo, Z. Single molecule studies of spliceosomal snRNAs u2-u6. in *Department of Chemistry Vol. Doctor of Phylosophy* (Wayne state Univedrsity, Detroit, Michigan, 2010).
35. Bae, E. et al. Structure and interactions of the first three RNA recognition motifs of splicing factor prp24. *J Mol Biol* **367**, 1447-58 (2007).
36. Karaduman, R. et al. Structure of yeast U6 snRNPs: arrangement of Prp24p and the LSm complex as revealed by electron microscopy. *RNA* **14**, 2528-37 (2008).
37. Pontius, B.W. & Berg, P. Rapid assembly and disassembly of complementary DNA strands through an equilibrium intermediate state mediated by A1 hnRNP protein. *J Biol Chem* **267**, 13815-8 (1992).
38. Portman, D.S. & Dreyfuss, G. RNA annealing activities in HeLa nuclei. *EMBO J* **13**, 213-21 (1994).

39. Herschlag, D. RNA chaperones and the RNA folding problem. *J Biol Chem* **270**, 20871-4 (1995).
40. Shannon, K.W. & Guthrie, C. Suppressors of a U4 snRNA mutation define a novel U6 snRNP protein with RNA-binding motifs. *Genes Dev* **5**, 773-85 (1991).
41. Jandrositz, A. & Guthrie, C. Evidence for a Prp24 binding site in U6 snRNA and in a putative intermediate in the annealing of U6 and U4 snRNAs. *EMBO J* **14**, 820-32 (1995).
42. Raghunathan, P.L. & Guthrie, C. A spliceosomal recycling factor that reanneals U4 and U6 small nuclear ribonucleoprotein particles. *Science* **279**, 857-60 (1998).
43. Brow, D.A. & Guthrie, C. Splicing a spliceosomal RNA. *Nature* **337**, 14-5 (1989).
44. Vidaver, R.M., Fortner, D.M., Loos-Austin, L.S. & Brow, D.A. Multiple functions of *Saccharomyces cerevisiae* splicing protein Prp24 in U6 RNA structural rearrangements. *Genetics* **153**, 1205-18 (1999).
45. Strauss, E.J. & Guthrie, C. A cold-sensitive mRNA splicing mutant is a member of the RNA helicase gene family. *Genes Dev* **5**, 629-41 (1991).
46. Ghetti, A., Company, M. & Abelson, J. Specificity of Prp24 binding to RNA: a role for Prp24 in the dynamic interaction of U4 and U6 snRNAs. *RNA* **1**, 132-45 (1995).
47. Martin-Tumasz, S., Reiter, N.J., Brow, D.A. & Butcher, S.E. Structure and functional implications of a complex containing a segment of U6 RNA bound by a domain of Prp24. *RNA* **16**, 792-804 (2010).

48. Martin-Tumasch, S., Richie, A.C., Clos, L.J., 2nd, Brow, D.A. & Butcher, S.E. A novel occluded RNA recognition motif in Prp24 unwinds the U6 RNA internal stem loop. *Nucleic Acids Res* (2011).
49. Kwan, S.S. & Brow, D.A. The N- and C-terminal RNA recognition motifs of splicing factor Prp24 have distinct functions in U6 RNA binding. *RNA* **11**, 808-20 (2005).
50. Hashimoto, C. & Steitz, J.A. U4 and U6 RNAs coexist in a single small nuclear ribonucleoprotein particle. *Nucleic Acids Res* **12**, 3283-93 (1984).
51. Cooper, T.A., Wan, L. & Dreyfuss, G. RNA and disease. *Cell* **136**, 777-93 (2009).
52. Wang, G.S. & Cooper, T.A. Splicing in disease: disruption of the splicing code and the decoding machinery. *Nat Rev Genet* **8**, 749-61 (2007).
53. Ward, A.J. & Cooper, T.A. The pathobiology of splicing. *J Pathol* **220**, 152-63 (2010).
54. Kalnina, Z., Zayakin, P., Silina, K. & Line, A. Alterations of pre-mRNA splicing in cancer. *Genes Chromosomes Cancer* **42**, 342-57 (2005).
55. Licatalosi, D.D. & Darnell, R.B. Splicing regulation in neurologic disease. *Neuron* **52**, 93-101 (2006).
56. Walter, N.G. Structural dynamics of catalytic RNA highlighted by fluorescence resonance energy transfer. *Methods* **25**, 19-30 (2001).
57. Aleman, E.A., Lamichhane, R. & Rueda, D. Exploring RNA folding one molecule at a time. *Curr Opin Chem Biol* **12**, 647-54 (2008).
58. Rueda, D. & Walter, N.G. Fluorescent energy transfer readout of an aptazyme-based biosensor. *Methods Mol Biol* **335**, 289-310 (2006).

59. Klostermeier, D. & Millar, D.P. Time-resolved fluorescence resonance energy transfer: a versatile tool for the analysis of nucleic acids. *Biopolymers* **61**, 159-79 (2001).
60. Zhao, R. & Rueda, D. RNA folding dynamics by single-molecule fluorescence resonance energy transfer. *Methods* **49**, 112-7 (2009).
61. Klostermeier, D. & Millar, D.P. RNA conformation and folding studied with fluorescence resonance energy transfer. *Methods* **23**, 240-54 (2001).
62. Selvin, P.R. Fluorescence resonance energy transfer. *Methods Enzymol* **246**, 300-34 (1995).
63. Roy, R., Hohng, S. & Ha, T. A practical guide to single-molecule FRET. *Nat Methods* **5**, 507-16 (2008).
64. Subasinghe, S.A.L.I. Wayne state University, Detroit, Michigan (2012).
65. Dexheimer, T.S., Stephen, A.G., Fivash, M.J., Fisher, R.J. & Pommier, Y. The DNA binding and 3'-end preferential activity of human tyrosyl-DNA phosphodiesterase. *Nucleic Acids Res* **38**, 2444-52 (2010).
66. Lakowicz, J.R. *Principles of fluorescence spectroscopy*, (Springer, 2006).
67. Aitken, C.E., Marshall, R.A. & Puglisi, J.D. An oxygen scavenging system for improvement of dye stability in single-molecule fluorescence experiments. *Biophys J* **94**, 1826-35 (2008).
68. Karunatilaka, K.S., Solem, A., Pyle, A.M. & Rueda, D. Single-molecule analysis of Mss116-mediated group II intron folding. *Nature* **467**, 935-9 (2010).
69. Tsai, R.T. et al. Spliceosome disassembly catalyzed by Prp43 and its associated components Ntr1 and Ntr2. *Genes Dev* **19**, 2991-3003 (2005).

70. Maeder, C., Kutach, A.K. & Guthrie, C. ATP-dependent unwinding of U4/U6 snRNAs by the Brr2 helicase requires the C terminus of Prp8. *Nat Struct Mol Biol* **16**, 42-8 (2009).

ABSTRACT**SPLICEOSOMAL PRP24 UNWINDS A MINIMAL U2/U6 COMPLEX FROM YEAST**

by

CHANDANI MANOJA WARNASOORIYA

May 2013

Co-Advisors: David Rueda and Louis J. Romano**Major:** Chemistry (Biochemistry)**Degree:** Master of Science

Splicing plays a major role in eukaryotic gene expression by processing pre-mRNA to form mature mRNA. Pre-mRNAs undergo splicing to remove introns, non-protein coding regions, and religate exons, protein coding regions. This process is catalyzed by the spliceosome, which consists of five small nuclear ribonucleoprotein particles (snRNPs: U1, U2, U4, U5 and U6) and numerous protein factors. Proper assembly of spliceosomal components is critical for function, and thus, defects in assembly can be lethal. Several spliceosomal proteins facilitate structural rearrangements important for spliceosomal assembly and function. Prp24 is an essential factor in U6 snRNP assembly, and it has been proposed to assist in U4/U6 formation and unwinding. Here, we address the question whether Prp24 affects the U2/U6 complex dynamics. Using single-molecule Fluorescence Resonance Energy Transfer (smFRET), we have previously shown that a minimal U2/U6 complex from yeast can adopt at least three

distinct conformations in dynamic equilibrium. Our new single molecule data show that Prp24 unwinds U2 from U2/U6 complex and stabilizes U6 in a low FRET conformation. We also show that the RNA Recognition Motifs of Prp24 affect the binding affinity of Prp24 for U6 and unwinding activity. We propose that Prp24 plays an important role in U2 and U6 snRNP recycling by dissociating the U2/U6 complex.

